Available online at www.sciencedirect.com
SCIENCE DIRECT®
Mechanical Systems and Signal Processing 20 (2006) 1953–1966
Mechanical Systems and Signal Processing
www.elsevier.com/locate/jnlabr/ymssp

Wheel-flat diagnostic tool via wavelet transform

Vittorio Belotti*, Francesco Crenna, Rinaldo C. Michelini, Giovanni B. Rossi

PMARLab Laboratory of Design and Measurement for Automation and Robotics, DIMEC-Department of Mechanics and Machines Design, University of Genova, Via all'Opera Pia, 15/A-16145 Genova, Italy

Received 19 November 2004; received in revised form 21 December 2005; accepted 24 December 2005
Available online 9 March 2006

Abstract

The detection and acknowledgement of *signatures*, for condition monitoring and fault diagnostics by wavelet transform, deserves increased attention, due to its property of variable time–frequency resolution, which overcomes limitations of classical time–frequency approaches.

In the paper, a diagnostic tool is presented, based on the wavelet transform, able to detect and to quantify the wheel-flat defect of a test train at different speeds and to measure the train speed with proper accuracy. The designed diagnostic tool minimises the hardware requirements, since only one accelerometer is needed, and provides results in real time.

The results, achieved by an exhaustive experimental campaign, permit to validate the effectiveness of the diagnostic tool and to demonstrate the advantages of wavelet-based detection of signatures.
© 2006 Elsevier Ltd. All rights reserved.

Keywords: Wavelet analysis; Fault diagnostic; Vibration measurement; Wheel-flat in railway; Signal processing

1. Introduction

In the railway transportation domain, the wheel–rail contact plays an important role: it could be considered the nodal point where the interests of infrastructure and vehicle managements meet together to assure passenger and freight traffic service. Moreover, the wheel–rail contact bears on other relevant aspects such as human and transportation reliability and environmental pollution. So, it is important to detect defects that deteriorate the wheel–rail contact, as soon as possible.

In this work, we have conceived and carried out a diagnostic tool capable to detect the most common 'localised wheel defect', the wheel-flat. The diagnostic tool efficiency is tested by an exhaustive experimental campaign, and its wide range of application is verified. Moreover, to estimate the defect severity, an algorithm for post-processing quantitative analyses is developed and implemented, which works with reasonably efficiency.

On the basis of the studies on time-dependent analysers [1,2] and their applications [3,4], this work implements the wavelet transform for detecting the wheel-flat typical signature from the acceleration signal: this avoids the use of both on-purpose sensors and time-consuming signal-processing technique [5,6].

*Corresponding author. Tel.: +39 010 353 2231.
E-mail address: v.belotti@dimec.unige.it (V. Belotti).

0888-3270/$ - see front matter © 2006 Elsevier Ltd. All rights reserved.
doi:10.1016/j.ymssp.2005.12.012

From an economical, safety and environmental point of view, the availability of a predictive on-process diagnostic, able to detect critical items before any dangerous deterioration, clearly, becomes a basic opportunity, avoiding the subsequent damage of the interfaced fixtures.

The present work starts with a short description of the wheel-flat fault and of its dynamics, and then presents the experimental set-up. Thereafter, we present the diagnostic tool algorithm and the results obtained applying the tool to the experimental data. Finally, the paper summarises the post-processing tool used to estimate the fault entity.

2. The wheel-flat fault

The wheel-flat fault [7–15] is the most common of 'localised surface defects', giving rise to a family of wheel damages. It is a planar spot on the rolling surface of the wheel, originated by wheel–rail sliding. This happens when an incorrect braking makes the wheel locking; the reason is ascribed to blocked, defective or poorly tuned brakes, or to poor wheel–rail adhesion for environmental adversity (rain, ice, etc.), or accidental pollution (grease, oil, etc.). A typical "measure" of this defect entity/gravity is the wheel-flat length, L in Fig. 1, which could affect wheel circumference from few tens up to some hundreds of millimetres.

The contact forces are quite high; therefore, damage and wear are consistently relevant, mainly due to the great weights involved in the rail traffic and to the hardness of rail and wheel materials. It is clear that the continuous repetitions of impacts on rail, together with the high forces involved, cause rapid deterioration of, both, rolling and fixed railway equipments. If ignored or underestimated, the fault will wear out materials up to the breakdown [7–10].

3. Dynamics of wheel-flat impact

The flat spot breaks off the steady revolving motion, due to sudden lack of material, until the inertia starts again steady rotation. An impact occurs each time the flattened zone approaches the railhead (Fig. 1). The result is a series of periodic pulses, timely applied at a different location of the rail.

The elasticity of rail plays an important role in the study of this impact. On the hypothesis of perfectly rigid rail, the wheel would "fall" till the end of wheel-flat is reached. Actually, the track resilience modifies the situation, and, at least, in a first range of speeds, the propagation of an elastic wave lowers the distance to the wheel when the "lack" of material is on it, since the railhead moves upwards [14,16].

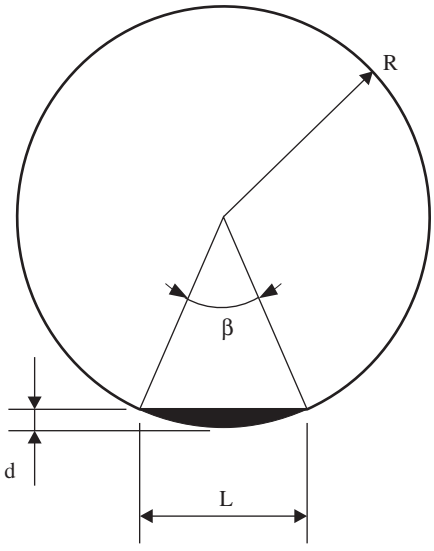

Fig. 1. Main quantities involved in the defect: d, wheel-flat depth; L, wheel-flat length; R, wheel radius; b, inner wheel-flat angle.

Indeed, depending on the train speed, the behaviour of the rail–wheel system in the presence of wheel-flat could be qualitatively divided as follows [17]:

(a) The impact force (thus, the damage and the noise generation) is proportional to the train speed up to a *critical speed*.
(b) The impact force becomes more or less constant, as the critical speed is passed.

The stabilisation of impact force is intuitively explained by the coupled motion of bodies with different inertias that makes the wheel to "fly out" the flatten zone.

The phenomena are properly studied by the technical literature. Refs. [17,18] provide convenient models, supported by results on a 1:8 scale model, describing the dynamics of different wheel–rail discontinuities. From the model, the critical speed is

$$v_c = \gamma[gR(1 + m_{\text{all}}/m_w)]^{1/2}, \tag{1}$$

where g is the gravity acceleration, R the radius of the wheel, m_w the mass of the wheel, m_{all} the portion of the spring-mounted car mass allocated to each wheel and γ a function depending mainly by rail geometry, material properties and foundation stiffness.

Under some further assumptions [17], and for typical values of the quantities in Eq. (1), we obtain that $\gamma \approx 2.2$ and, then, within the data of the present study, the critical speed is found to be $v_c \simeq 50\,\text{km/h}$.

The force behaviour above the critical speed is reckoned by the total change of momentum of the impacting wheel that, under the cited model approximations, is independent from the train speed and is equal to

$$2m_{eq}\omega_1 z_1[1 - (1 - d/z_1)^2]^{1/2}, \tag{2}$$

where m_{eq} is the equivalent rail mass, ω_1 the first resonance of the rail, d the wheel-flat depth and z_1 the static deflection of the rail under wheel load.

Summing up, the recalled studies lead to the two useful results: the determination of critical speed and low dependence of the impact force from train speed. The exposed and other literature Refs. [7,12,14,15] make us confident to set up a threshold-based diagnostics and to look after a condition-monitoring maintenance set-up for on-duty trains.

4. Experimental set-up

An experimental layout was designed, to provide the information, to develop and to validate a reliable, effective and low-cost wheel-flat diagnostic tool. The measurement set-up avails of a testing train with wheels having different degrees of damage and an instrumented rail track. For these tests, the Italian Railway Workshop of Florence artificially produced the flats, which could be considered as new wheel-flat defects: they have sharp edges on the corner.

The train composition is as follows:

- one electric locomotive E646 for passenger transport, without wheel defects;
- three testing passenger car cabs MDVC[1] with defected wheels, as shown in Fig. 2;
- one ending cab npBD,[2] without wheel defects.

The rail is instrumented with four accelerometers and an inductive axle-counter block. All data are acquired with a sampling frequency of 12.8 kHz and are digitally converted by a 12-bit acquisition board. The instrumented rail map and the testing train are represented in Fig. 2. The experiment set-up and organisation are made in collaboration with the National Railway Company and the University of Firenze.

[1]Medium distance cars with middle doors.
[2]Push–pull control car with lowered plane.

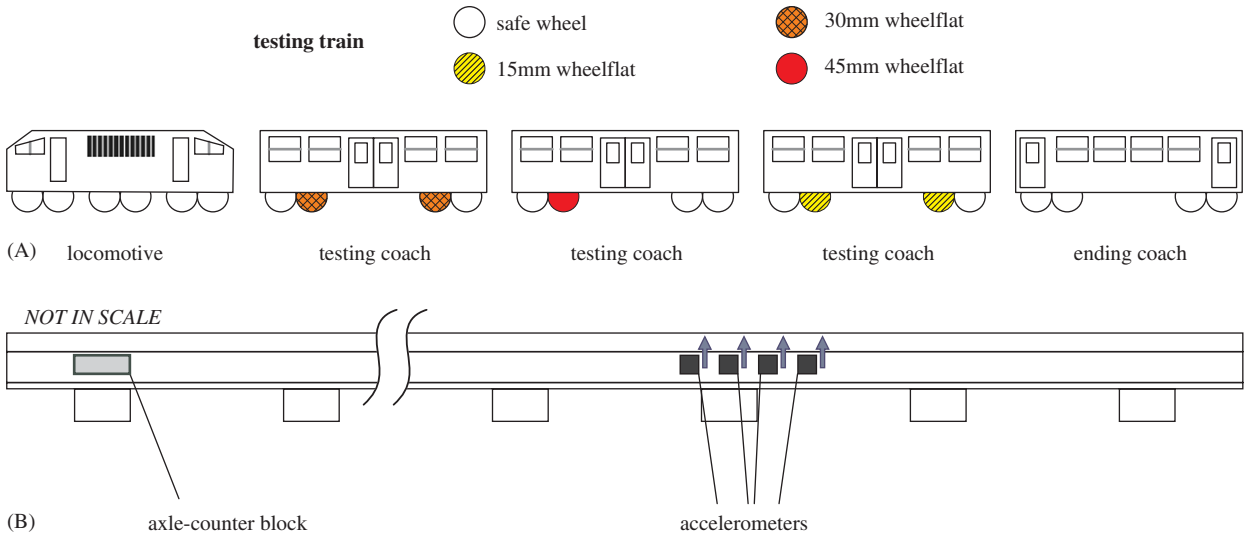

Fig. 2. (A) Testing train scheme with damaged wheels represented as shown in the above legend and (B) instrumented rail where the arrows near the accelerometers indicate their measuring axes (figures are not in scale).

The overall measurement campaign provides a total of 50 test signals in different testing configurations: train speed from 10 km/h up to 100 km/h, with an increasing step of 10 km/h and in both directions. For each test, all four accelerometric signals are collected, but in the present study, only one has been used.

Beside that, another set of acceleration signals is available with different coaches set-up and a blind configuration of defects.

4.1. The acquired data

A typical time history of the acquired acceleration signal is shown in Fig. 3. The acceleration peaks are generated, both, by the wheel-flat impact and the wheel transit above the accelerometer. The high number of peaks present in the signal is the evidence that for each fault, not only the impact recorded by the sensor is the one that occurs nearby the accelerometer, but also farther impacts superimpose as well.

The spectral content of the signal is noisy and about 70% of the signal energy is typically limited in the frequency region up to 2 kHz; no characterising frequency signature could be retrieved from the spectrum. The complexity of the fault spectral content is also acknowledged by the few works on wheel-flat detection present in the literature [5,6]. In these works, the fault detection is not based on the extraction of a typical frequency signature, but it exploits the detection of the repetition of the impacts: the analysed rail acceleration signal need be acquired by an on-purpose piezoelectric sensor; the algorithm procedure is quite complex and it includes many different signal-processing (filtering, Hilbert transforms, unbiased autocorrelation and power spectral density) schemes, before reaching acceptable reliability.

5. The diagnostic tool and the experimental results

5.1. Diagnostic tool basic specifications

As previously depicted, the aim of this research is to build a diagnostic tool able to identify a wheel-flat-damaged wheel from the rail acceleration signal, by a sound and a simple procedure. In addition, after the wheel-flat detection, the diagnostic instrument should be able to quantify the entity of the wheel-flat damage.

The wanted diagnosis should detect not only the train with one or more damaged wheels but we also want to single out the exact bogie. On knowing the damaged bogie, the respective coach will be removed from the train and sent to the maintenance shop for the bogie remediation. This purpose together with the use of a

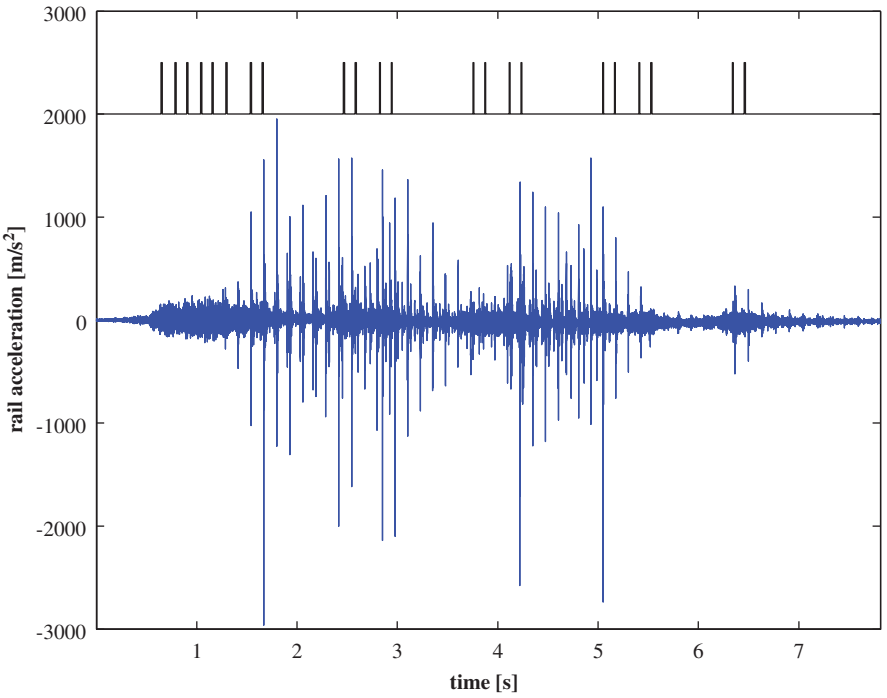

Fig. 3. Rail acceleration measured by one accelerometer during a train pass-by at the speed of 19.4 m/s (70 km/h); the axle-counter block signal is plotted at the top in arbitrary units.

unique accelerometer makes useless overall analysis; indeed, only a time-dependent analysis could correlate the acceleration peaks in Fig. 3 with each wheel transit above the sensor.

The choice of the analyser, taken to process data, characterises the behaviour and the on-duty specifications of the diagnostic tool. Let begin by the wanted requisites for the analyser: sufficient time resolution to single out the damaged bogie; capability of the on-line detection of the defect, and minimisation of false alarms (both false positive and false negative).

The time resolution necessary for our application is 0.09 s, i.e. the time half-interval between two consecutive bogies at the highest train speed reached in the tests (the distance between the bogies of two adjacent coaches is about 5 m, which is covered in 0.18 s at the maximum speed of 27.8 m/s, i.e. 100 km/h). Indeed, this specification could be relaxed with constraints on the train speed.

The on-line defect detection condition needs a signal-processing computation time as fast as possible; coach pass-by time at the minimum testing train speed is about 10 s, which corresponds to about 130 k sample for coach at the testing sample frequency. Thus, the analyser computation algorithm should be assumed to have the consistent processing time.

Finally, low cost, toughness and steady performance are common requisites, which every diagnostic tool should apply to, especially when used in outdoor stands.

5.2. Analyser choice

As previously exposed, the diagnostic tool should be able to identify and extract the wheel-flat signature from the acquired signal. In Refs. [1,2], studies are reported performed on the characterisation of some time-dependent analysers: both time–frequency and time–scale. For an exhaustive theory on the time-dependent analysers, their estimation and their properties, we defer to [19–22].

The signature extraction capability, the studies and the applications in the literature [1–4], the exposed diagnostic specification and the signal characteristics, all four facts drive the choice of analyser based on the discrete wavelet transform (DWT).

The key advantage of wavelets for our application is the multi-resolution property: the information enclosed in the signal is splitted at different levels. The wavelet-level selection permits to distinguish the train property we want to investigate, such as axle transit or wheel defect, assuring high flexibility to the diagnostic tool. This means that the suitable choice of the wavelet package makes possible to detect the desired information, spread by levels, in a single analysis.

Summing up, the DWT provides effective analysing properties for the sought diagnostic tool: the spectral-content splitting-property leads to extract specialised signatures and the dyadic computation algorithm grants the signal-processing quickness.

The asymmetric shape produced by the impulsive impact acceleration drives us to select the fourth-order Daubechies [23] wavelet as mother wavelet: its orthogonality grants that the wavelet atoms are a base for the time–scale space. Besides, the orthogonal property assures the minimum number of operations to compute the transform. The wavelet function and its scaling function are shown in Fig. 4.

We recall the continuous wavelet transform $W_x(a,b;\psi)$ of the signal $x(t)$ defined by

$$W_x(a,b;\psi^*) = \int x(t)\,\frac{1}{\sqrt{a}}\psi\left(\frac{t-b}{a}\right)\mathrm{d}t, \tag{3}$$

where a is the scale parameter, b the time parameter and $\psi*(\cdot)$ the complex conjugate of the mother wavelet $\psi(\cdot)$.

In the DWT, the scale and time parameters should vary according to the positions:

$$a = 2^m, \ \text{dyadic scale}; \quad b = na = 2^m n, \ \text{dyadic shift} \tag{4}$$

with $n,m \in \mathbb{N}$, where m is called the *wavelet level*.

It immediately follows from positions (4) that low levels (small m) correspond to low scale (small a); hence, these are mostly affected by the high-frequency content of the signal. The other way around, the low-frequency content of the signal mostly contributes to the high-level coefficients of the wavelet transform.

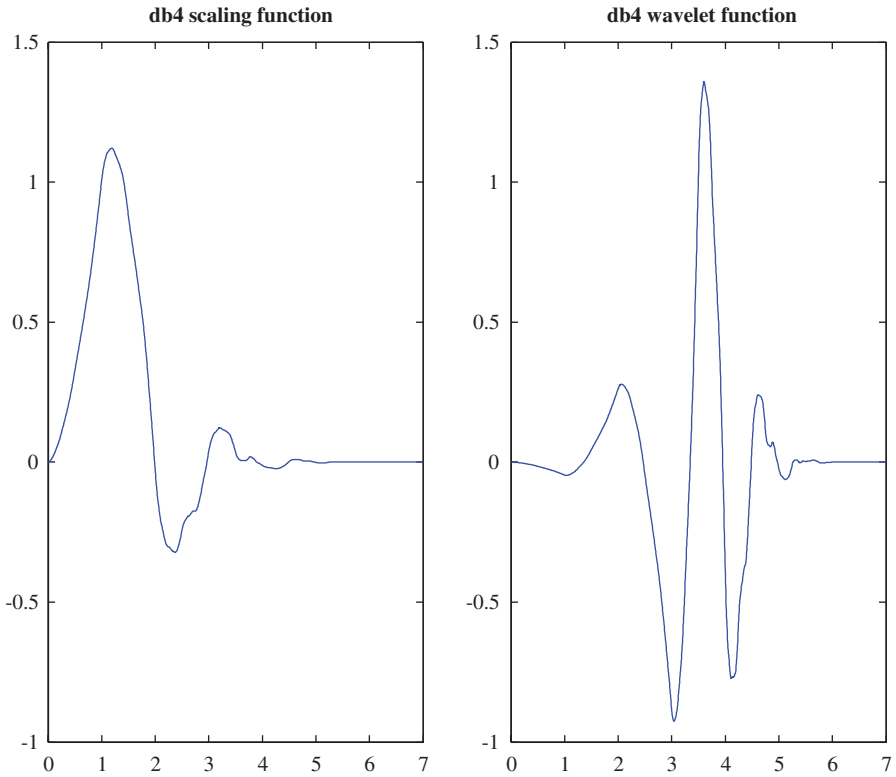

Fig. 4. Daubechies fourth-order scaling and wavelet function.

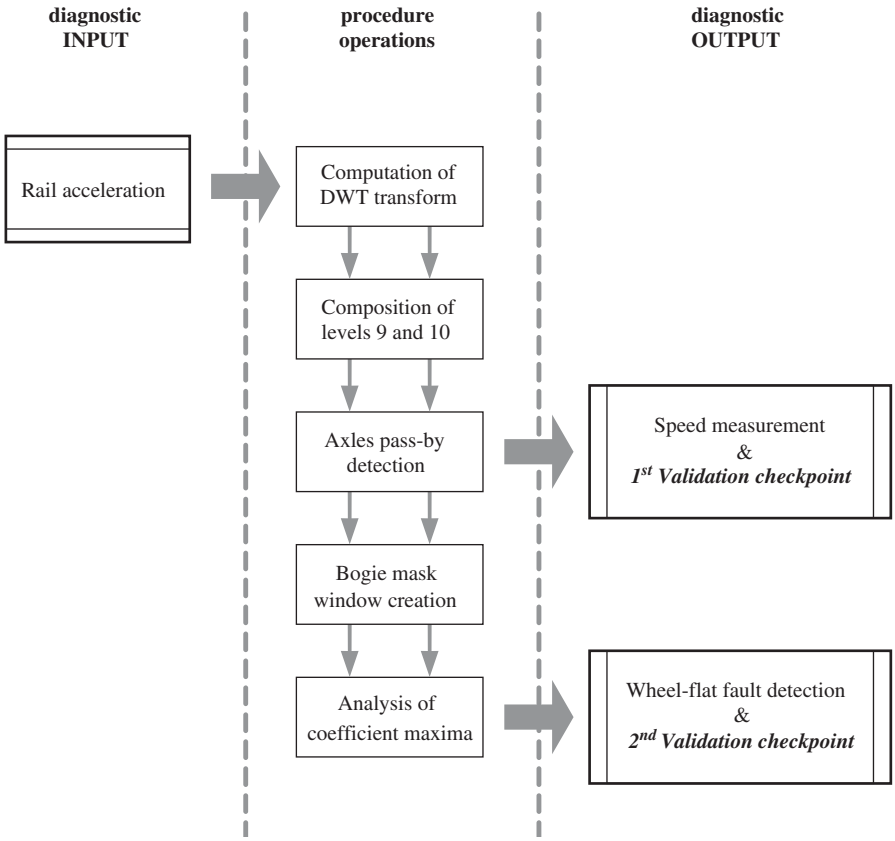

Fig. 5. Flow chart of wheel-flat detection procedure: the diagnostic tool inputs are on the left and the outputs are on the right; in the middle there are the procedure operations sequence. The two points of the validation procedure are also shown in the figure.

The DWT could also be thought as the orthogonal projection of the signal $x(t)$ in the time–scale space[3]:

$$W_x(a,b;\Psi) = \langle x, \Psi_{a,b} \rangle, \tag{5}$$

where $\psi_{a,b}$ is the wavelet function b-shifted and a-scaled with the parameters a and b according to the positions expressed in Eqs. (4).

5.3. Overview of the detection procedure

The diagnostic procedure's basic idea is to use a single accelerometer, solid to the rail, in view of assessing, both, the train speed and the wheel health status. A flow chart of the detection process is sketched in Fig. 5; each step will be presented together with the application to the experimental investigation.

In order to prove the validity of the whole procedure, we set two validation checkpoints: the first, at the train speed measurement and the other, at the wheel-flat detection.

These two validation points also split the procedure in two parts. In the first part, we use the high levels of the wavelet transform of the acceleration signal; thus, we use the low-frequency signal content. From these coefficients, the transit of each axle over the accelerometer is detected and the train speed is measured.

In the second part, we use the low-level coefficient of the wavelet transform of the acceleration signal; thus, we investigate its high-frequency content. Using these coefficients, jointly with the axle transit information achieved in the first part, we detect, for each coach, the bogie that contains wheel-flat-damaged wheels.

[3]The symbol $\langle f, g \rangle$ denotes the scalar product of f with g.

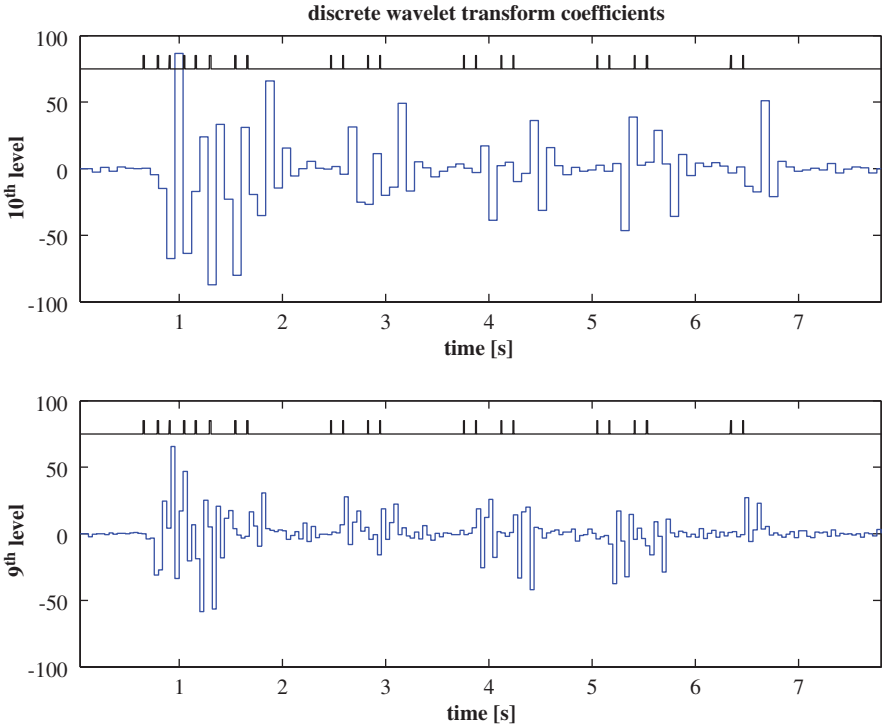

Fig. 6. Graph of coefficients of levels 10 and 9 of the DWT of the signal in Fig. 3; the axle-counter block signal is plotted at the top of each subfigure in arbitrary units.

5.4. Axle transit detection

The axle transit over the accelerometer is a useful information used to focus the defect detection algorithm. Although the axle-counter block provides such pass-by information, we found the alternative to obtain it by the wavelet transform of the signal. In this way, the axle-counter block is no more necessary and this is an evident economical benefit for the diagnostic tool; besides that, the axle counter becomes now a validating signal.

At the present sampling frequency, the tenth wavelet level is the highest one at which it is possible to distinguish two different nearby bogies at the maximum speed.[4] The procedure starts computing the DWT of the rail acceleration and the wavelet coefficients of the first's 10 levels are stored, waiting to be processed. Higher sampling frequency is required for fast travelling trains, but these conditions are normally avoided, as the measurement stands are usefully located in the proximity of stations, where trains slow down.

Then, the two levels, the ninth and the tenth (Fig. 6), are composed together to create the axle pass-by signal, as shown in Fig. 7: using the coefficients and the wavelet inverse-transform we obtain two reconstructed signals with the same time resolution of the acquired data, and then their absolute values are added together.

Each peak of Fig. 7 corresponds to the axle transit over the accelerometer: the first's six peaks are the locomotive axles transit, and then there are the four coaches with four axles each. The train speed, i.e. the first tool output, is measured from this signal computing the time separation between peaks.

For each coach, from the axle pass-by signal, we measure the time separation between inner-axles; then, the coach speed is computed using the known inner-axles distance of 16.6 m. From the axle-counter block, the

[4]As previously told, the necessary time resolution is 90 ms: the time resolution for the tenth wavelet level is 80 ms with a sampling frequency of 12.8 kHz.

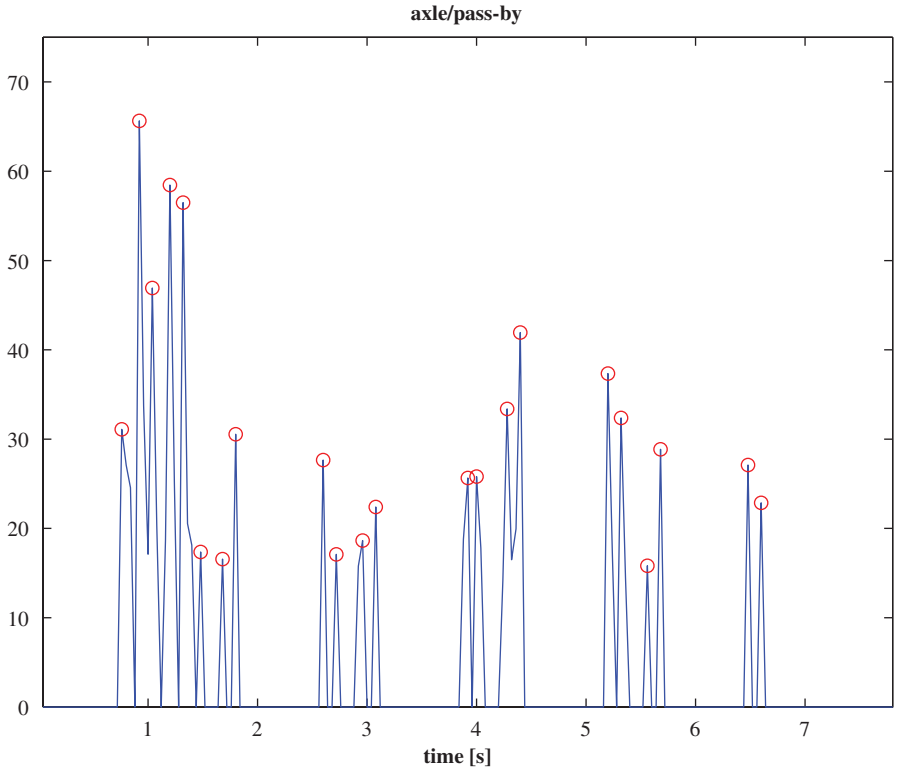

Fig. 7. Axle pass-by signal created starting from the coefficients of Fig. 6; circles indicate the axle transit found out by a maxima-search algorithm.

Table 1
Results of weighted speed-difference, $\Delta V/V$ in Eq. (6), at different nominal train speeds

Train speed (km/h)	10	20	30	40	50	60	70	80	90	100
$\Delta V/V$ mean (%)	0.31	0.36	0.29	0.20	0.13	0.02	0.29	0.44	0.02	0.17
$\Delta V/V$ standard deviation (%)	0.03	0.27	0.14	0.73	0.58	0.35	0.65	0.32	0.84	0.90

coach speed is also computed and this is used as *reference* speed. Since the speed is measured for each coach and for all tests, we have a good statistics[5] to verify this train speed measurement via the wavelet transform.

Moreover, to verify the efficiency at different train speeds of these measurements via wavelet transform, for each coach, we calculate the weighted speed-difference given by

$$\Delta V/V = |V_{\mathrm{ACB}} - V_{\mathrm{DB4}}|2/(V_{\mathrm{BCA}} + V_{\mathrm{DB4}}), \tag{6}$$

where V_{ACB} is the reference speed obtained by the axle-counter block sensor and V_{DB4} the one obtained by wavelet axle pass-by signal. The results, given in Table 1 ordered by train speed, show that the exposed speed measurements via wavelet transform can replace the use of the axle-counter block without loss on information. We again note that the train nominal speed of 100 km/h is the maximum measurable speed with the wavelet transform at the current sample frequency[6]; to measure higher train speed, the sample frequency should be incremented.

[5] 50 tests × 4 coaches = 200 speed measurements.

[6] Bogie axles distance is 2.4 m, then the axle time separation at 100 km/h is 86 ms: this value is very close to 80 ms ($= 2^{10}/12.8$ kHz) that is the time resolution of wavelet transform at tenth level.

5.5. Wheel-flat detection

Before going on with the procedure, it is important to notice that with only one accelerometer signal, it is impossible to detect which axle of a bogie is damaged; in fact, the bogie axles distance is 2.4 m while the wheel circumference is 2.8 m, yielding the two circumference extensions to superimpose. From a diagnostic and economical viewpoint, this is not a problem at all: if a wheel of a coach is damaged, the all coaches shall be moved to the maintenance shop. Then the maintenance activity will be directed towards the indicated defected bogie. It is sufficient to detect the bogie with the wheel-flat defected wheel, rather than the wheel itself.

The validated axle pass-by signal, obtained in the previous procedure step, is now used to create the *bogie-mask* window. This is a window in the time domain, exploited to synchronise the wheel-flat detection and bogie transit over the accelerometer. The bogie-mask synchronisation is needed to focalise the detection algorithm minimising the false alarm that could be generated by the wheel-flat impact repetitions on the rail. The bogie-mask window will cut off everything outside the bogie transit and will leave unchanged the signal inside it.

In Fig. 8, the bogie-mask window is presented together with the generating axle pass-by signal. Each bogie transit is centred using the respective two axle transit instants (indicated by circle in the figure). The single bogie window length, namely the time for which it is equal to one, corresponds to a single wheel circumference at the train speed computed as previously exposed. This length grants to analyse only the wheel-flat acceleration peak nearest to the accelerometer (if there is).

The wheel-flat detection is achieved with the last step of the procedure. Preliminary tests on the data showed the wheel-flat damage signature is mainly splitted by the DWT in the fourth-level coefficients. From the same tests, the threshold level was settled according to the experimental data.

The definitive wheel-flat detection procedure uses the fourth-level coefficients and the bogie-mask window to carry out a single value for each bogie. This value is compared to the threshold, in order to state if the bogie

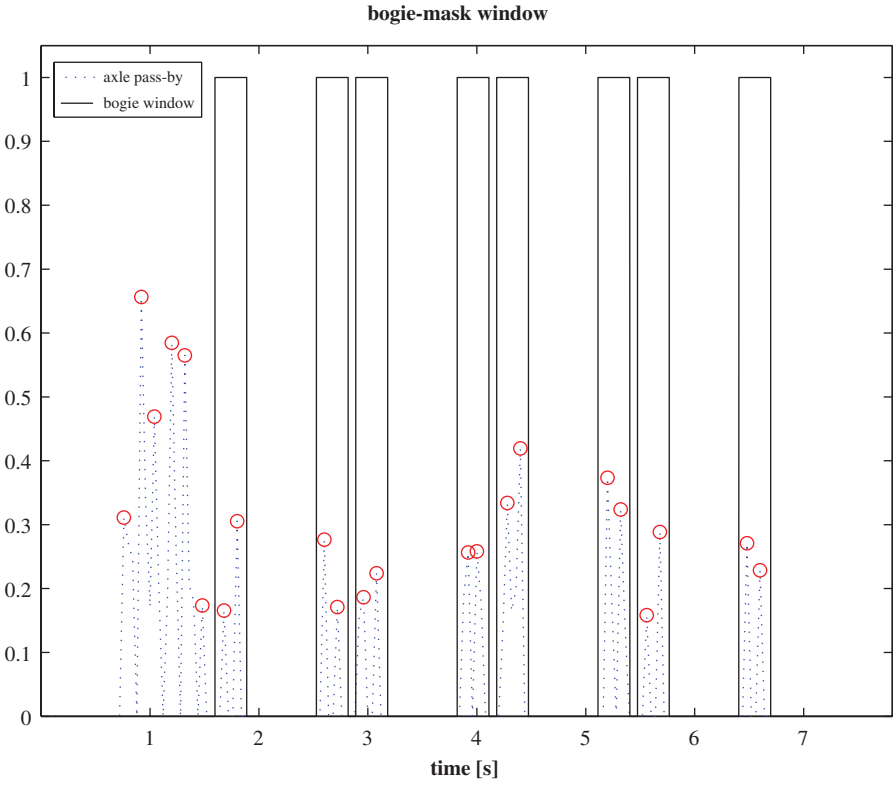

Fig. 8. Graph of the bogie-mask window (solid line) generated using the signal in Fig. 7 (dotted line, 1/100 scaled).

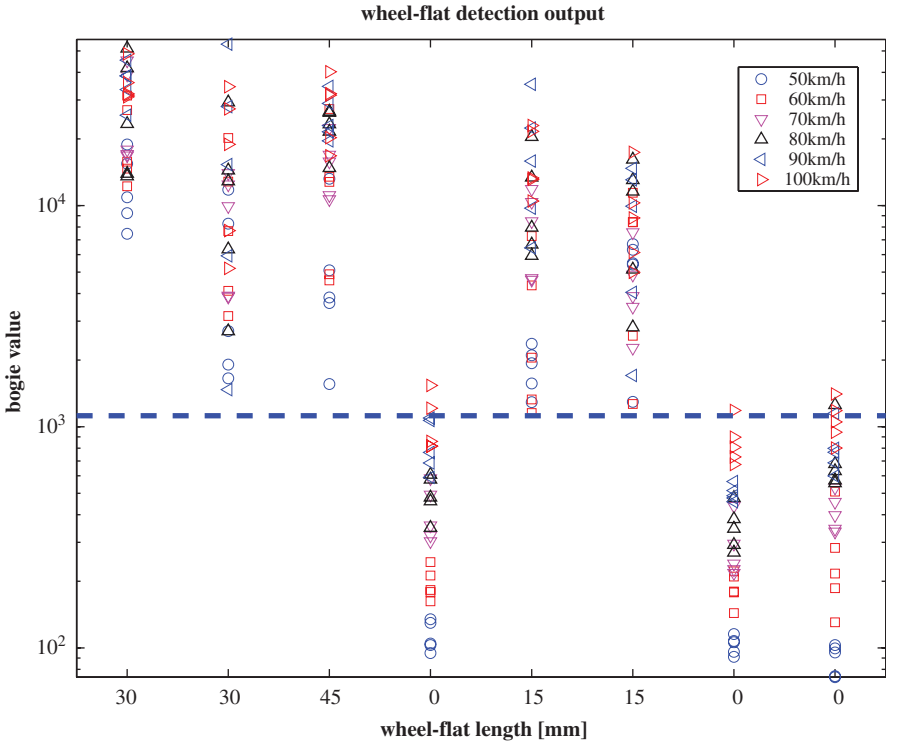

Fig. 9. Wheel-flat detection output for all bogies of train with a speed from 50 to 100 km/h. The dashed line indicates the threshold value. The use of logarithmic scale is needed to clearly see the threshold zone and the non-defected bogie values. The x-axis reports the boogies sequence sorted by the train composition as illustrated in Fig. 2A.

includes wheel-flat-damaged wheels. In Fig. 9, the bogie values are plotted for all bogies analysed, distinguished by speed and wheel-flat length.

Even if not in the purposes of this work, it can be noted that non-defected wheels present coefficients increasing with the train speed; while the defected ones obtain diagnostic values not sorted by speed, according to the model theory. Moreover, the not-strictly dependence of diagnostic results from wheel-flat length agrees with the idea of searching a signature that is typical of the defect and could not be linked to its entity.

To validate the exposed guesses, the procedure is applied to all trains, with a speed from 50 km/h (the critical speed) to 100 km/h. A total of 240 bogies[7] are dealt with and our diagnostic tool detected all the 150 damaged bogies. The complete diagnostic tool performance rate is shown in Table 2. The diagnostic tool also generates seven false alarms, but if the train speed range were limited to about 90 km/h, only two false alarms would be generated.

Varying the threshold value of $\pm 10\%$ and verifying how results modify, we test the detection performance robustness. As shown in Table 3, the prospected detection procedure is quite robust to threshold variation; this indicates the stability of the diagnostic tool performance. Moreover, the same diagnostic procedure is also tested with the experimental data with different train set-up and blind defect configuration; it maintains the same detection performance.

6. Wheel-flat damage estimation

The dependence of the impact force from the wheel-flat depth is not linear, as shown in model Eq. (2); the wheel-flat length and depth are related by trigonometric functions that are not linear as well. At last, more complex model [14] should be considered to take in account other non-linearity of the wheel-flat phenomena.

[7] 2 bogies × 4 coaches × 6 train speeds × 5 test repetitions = 240 bogies (150 defected, 90 safe).

Table 2
Results of wheel-flat detection at different nominal train speeds (km/h) (the ratio indicates the number of bogies detected as damaged on the actually defected bogies)

Coach number	*Bogie state*	Train speed (km/h)					
		50	60	70	80	90	100
1	30 mm	5/5	5/5	5/5	5/5	5/5	5/5
1	30 mm	5/5	5/5	5/5	5/5	5/5	5/5
2	45 mm	5/5	5/5	5/5	5/5	5/5	5/5
2	Safe	0/0	0/0	0/0	0/0	0/0	2/0
3	15 mm	5/5	5/5	5/5	5/5	5/5	5/5
3	15 mm	5/5	5/5	5/5	5/5	5/5	5/5
4	Safe	0/0	0/0	0/0	0/0	0/0	1/0
4	Safe	0/0	0/0	0/0	1/0	1/0	2/0

Table 3
Variation of detection performance for train speed between 50 and 90 km/h by threshold modification

Threshold level (%)	Damaged bogies correctly detected (%)	Safe bogies detected as damaged (%)	Damaged bogies not detected (%)
−10	100.0	6.7	0.0
Nominal	100.0	2.7	0.0
+10	96.8	1.3	3.2

This high non-linearity between the impact force and the wheel-flat length it is difficult to quantify the damage entity; hence, some constraints should be applied to diagnostic quantification procedure as follows.

Italian railways consider dangerous a wheel-flat length greater than 40 mm and send the coach to the maintenance shop for wheel regeneration; so we set up a wheel-flat entity estimation keeping the following wheel classification:

- *Softly damaged*: The wheel-flat length is less than 40 mm, then the coach could stay on duty.
- *Heavily damaged*: The wheel-flat length is 40 mm or more, then the coach should go to maintenance.

Due to the above-mentioned non-linearity in the wheel-flat length estimation from the rail acceleration signal, we arrange the entity quantification procedure for trains with a speed of 90 km/h. In practice, the choice of *standard* train speeds for the wheel-flat damage estimation is not a limitation, in view of a reference diagnostic tool.

The quantitative estimation procedure applies off-line, only on the bogie classified as damaged by the real-time wheel-flat detection procedure. From the wavelet coefficients, computed by the wheel-flat detection procedure, we calculate the energy per bogie and per scale. This energy value is compared to a threshold level, optimised with experimental data, in order to classify the bogie as softly or heavily damaged.

At the train speed of 90 km/h, we have the data acquired from five train transits for a total of 25 defected bogies: five bogies heavily damaged with a 45 mm wheel-flat length; 10 bogies softly damaged with a 30 mm wheel-flat length and 10 bogies softly damaged with a 15 mm wheel-flat length.

The result of the computation provided noteworthy issues: four heavily damaged bogies and 19 softly damaged ones were correctly classified; the remaining two, one per type, obtained wrong damage estimation. The energy content of the wavelet signatures at the picked resolution level does not, possibly, provide unambiguous assessments, and the algorithm shall embed more (or more specific) information. Basically, one should remove the extra-energy, not dependent on the individual wheel-flat, rather on distributed noise;

suitable procedures based on the careful shaping of the wavelet package are under investigation, to define an effective feature-driven detection algorithm.

7. Conclusions

As foreseen by the preliminary design of the diagnostic tool, the discrete wavelet transform is very effective for the application. A peculiarity of the prospected diagnostic tool is the high efficiency in detecting all the damaged wheels and, as well, in measuring the train speed up to our purpose with a single rough sensor set-up. The conceived fault detection diagnostic procedure is validated by the results collected through the properly extended experimental campaign, and by the recalled dynamic model of wheel–rail system.

With the aim of applying the tool in an outdoor on-line measurement stand, all the diagnostic components, from sensors to the data-processing algorithms, are thought to satisfy high robustness and suitable low-cost requisites.

The resort to wavelet-based signatures may be especially relevant, in view of quantitative damage assessments, which anyway was not the primary purpose of this investigation. We rather pursued the development of an effective, reliable and cheap wheel-flat detector; the use of adaptable means was favoured, and the multi-resolution versatility, with the Daubechies wavelets neutrality, appeared winning option, as for flexibility, and as for effectiveness. The choice was, finally, successful, even leading to a set of preliminary quantitative estimations, in due agreement with the existing wheel-flats.

Once the primary purpose was achieved, the extension towards quantitative assessments was considered, since the theory properly suggests a one-to-one connection between flat spot extension and vibro-acoustic emission; a scale, built on the energy content of well-conditioned signatures, should single out the information strictly linked to each damage. To remove the noticed ambiguities, a different construction of wavelet signatures has to be followed, selecting a wavelet-packet, suitably put together, to select the all wheel-flat power and reject unrelated nuisances.

Acknowledgements

This research has been carried out with a grant of the Italian Research Ministry, MURST, as National Research Program in collaboration with the DMTI Research Group of University of Firenze.

References

[1] V. Belotti, F. Crenna, R.C. Michelini, G.B. Rossi, Time evolutionary analysis: Operator driven paradigms for fault diagnosis, in: Proceedings of the Third IEEE International Symposium on Diagnostics for Electrical Machines, Power Electronics and Drives, Grado (Gorizia), Italy, 2001, pp. 253–258.

[2] V. Belotti, F. Crenna, R.C. Michelini, G.B. Rossi, Metrological characterisation of time–frequency and time–scale analysers, in: Proceedings of the XVI IMEKO World Congress, Wien, Austria, vol. 5, 2000, pp. 7–12.

[3] G. Dalpiaz, A. Rivola, Condition monitoring and diagnostics in automatic machines: Comparison of vibration analysis techniques, Mechanical Systems and Signal Processing 11 (1997) 53–73.

[4] Z.K. Peng, F.L. Chu, Application of the wavelet transform in machine condition monitoring and fault diagnostics: A review with bibliography, Mechanical Systems and Signal Processing 18 (2004) 199–221.

[5] A. Bracciali, G. Lionetti, M. Pieralli, Effective Wheel Flats Detection Through a Simple Device, Techrail Workshop, Paris, 2002 (on CD).

[6] A. Bracciali, G. Cascini, M. Pieralli, The railway wheel-sets. Part 2 development of a detecting device, Ingegneria Ferroviaria 8 (2000) 511–520 (in Italian).

[7] J. Jergéus, C. Odenmarck, R. Lundén, P. Sotkovszki, B. Karlsson, P. Gullers, Full-scale railway wheel-flat experiment, Proceedings of the Institution of Mechanical Engineers. Part F—Journal of Rail and Rapid Transit 213 (1) (1999) 1–13.

[8] J. Ahlstrom, B. Karlsson, Microstructural evaluation and interpretation of the mechanically and thermally affected zone under railway wheel-flats, Wear 232 (1999) 1–14.

[9] C. Roberts, H.P.B. Dassanayake, N. Lehrasab, C.J. Goodman, Distributed quantitative and qualitative fault diagnosis: Railway junction case study, Control Engineering Practice 10 (2002) 419–429.

[10] M. Wallentin, H.L. Bjarnehed, R. Lundén, Cracks around railway wheel flats exposed to rolling contact loads and residual stresses, Wear 258 (7–8) (2005) 1319–1329.

[11] A. Johansson, J.C.O. Nielsen, Out-of-round railway wheels—wheel–rail contact forces and track response from full-scale measurements and numerical simulations, Proceedings of the Institution of Mechanical Engineers. Part F—Journal of Rail and Rapid Transit 217 (2003) 135–146.
[12] S.G. Newton, R.A. Clark, Investigation into the dynamic effects on the track of wheelflats on railway vehicles, Journal of Mechanical Engineering Science 21 (4) (1979) 287–297.
[13] T. Kigawa, E. Kimoto, Influences of skidding pattern upon the occurrences of skid damage to railway wheels, Wear 167 (2) (1993) 143–154.
[14] T.X. Wu, D.J. Thompson, A hybrid model for the noise generation due to railway wheel flats, Journal of Sound and Vibration 251 (1) (2002) 115–139.
[15] J.C.O. Nielsen, A. Johansson, Out-of-round railway wheels—a literature survey, Proceedings of the Institution of Mechanical Engineers. Part F—Journal of Rail and Rapid Transit 214 (2) (2000) 79–91.
[16] J.C.O. Nielsen, A. Igeland, Vertical dynamic interaction between train and track influence of wheel and track imperfections, Journal of Sound and Vibration 187 (5) (1995) 825–839.
[17] I.L. Vér, C.S. Ventres, M.M. Myles, Wheel/rail noise—Part III: Impact noise generation by wheel and rail discontinuities, Journal of Sound and Vibration 46 (1976) 395–417.
[18] P.J. Remington, Wheel/rail noise—Part I: Characterization of the wheel/rail dynamic system, Journal of Sound and Vibration 46 (1976) 359–379.
[19] M.B. Priestley, Spectral Analysis and Time Series, Academic Press, New York, 1981.
[20] M.B. Priestley, Non Linear and Non Stationary Time Series Analysis, Academic Press, New York, 1988.
[21] S. Mallat, A Wavelet Tour of Signal Processing, Academic Press, New York, 1998.
[22] M. Vetterli, M. Kovacevic, Wavelet and Subband Coding, Prentice-Hall PTR, Englewood Cliffs, NJ, 1995.
[23] I. Daubechies, Ten lectures on wavelets, in: CBMS-NSF Regional Conference Series in Applied Mathematics, vol. 61, SIAM, Philadelphia, PA, 1992.